Scaling Behaviour of Pressure-Driven Micro-Hydraulic Systems

N.R. Tas, T.S.J. Lammerink, J.W. Berenschot, M. Elwenspoek, A. van den Berg

MESA+ Research Institute, University of Twente,
P.O. Box 217, 7500 AE Enschede, The Netherlands
N.R.Tas@el.utwente.nl

ABSTRACT

This paper presents a lumped network approach for the modelling and design of micro-hydraulic systems. A hydraulic oscillator has been built consisting of hydraulic resistors, capacitors and transistors (pressure controlled valves). The scaling of micro-hydraulic networks consisting of linear resistors, capacitors and inertances has been studied. An important result is that to make smaller networks faster, driving pressures should increase with reducing size.

Keywords: scaling, micro-fluidics, hydraulic oscillator.

1 INTRODUCTION

Micro-hydraulic systems can be modeled and designed using a generalized physical system description [1, 2]. This approach is based on the assumption that it is possible to separate and concentrate properties of a system into interconnected subsystems. It has proven its great value in the design of electronic circuits. The lumped network approach also offers a powerful design tool for microfluidic systems [3-5]. To illustrate the far-reaching analogy between different physical domains, we have rebuilt an electronic astable multivibrator network in the hydraulic domain [4]. The system consists of hydraulic capacitors, resistors, transistors and (parasitic) coils. Based on this micro-hydraulic system the scaling behaviour of low *Re* (Reynolds number) hydraulic systems has been analyzed.

2 HYDRAULIC FUNDAMENTALS

In every physical domain a conserved quantity q can be distinguished [1]. The *flow* is the rate of exchange of this conserved quantity between subsystems. In the hydraulic domain the flow variable is the volume flow ϕ_V [m^3s^{-1}]. The *effort* is the tension that governs the exchange of the conserved quantity between subsystems. In the hydraulic domain the effort variable is the pressure p [Pa].

2.1 Hydraulic Resistors

The hydraulic resistor physically is a liquid flow restriction, symbolically represented as in fig. 1a. For a linear flow resistor, the resistance R is defined by:

$$R = \frac{p_{12}}{\phi_V} \qquad [\mathrm{N{\cdot}s{\cdot}m^{-5}}] \qquad (1)$$

Where $p_{12} = p_1 - p_2$ is the pressure drop across the resistor, and ϕ_V the volume flow through the resistor. At sufficient low *Re* the flow in a duct is laminar and fully developed (Poisseuille flow), and the pressure drop p across the duct is proportional to the volume flow rate ϕ_V. For a duct of arbitrary cross section the resistance is given by [6]:

$$R = \frac{2 \cdot f \cdot Re \cdot L \cdot \mu}{D_h^2 \cdot A} \qquad (2)$$

Where f is the Fanning friction factor, L is the length of the channel, μ is the viscosity of the liquid, D_h the hydrodynamic diameter, and A the cross sectional area. For a laminar fully developed flow the product $f{\cdot}Re = k$, a dimensionless constant only depending on the shape of the cross section. The hydraulic resistors we have tested, were realized by anisotropic KOH-etching into a <100> silicon wafer and closing of the channel by anodic bonding of a glass wafer onto the silicon. Fig. 1b-d show a side view, a cross section and a top view of the implemented restrictions respectively.

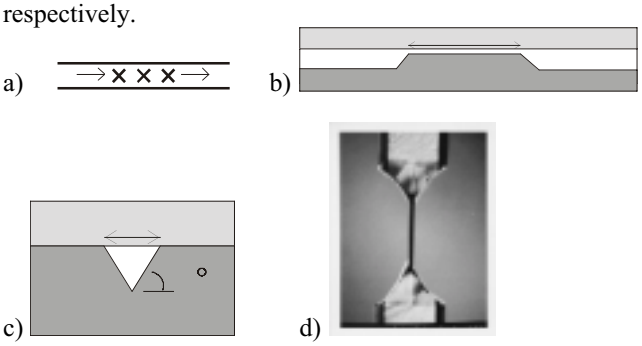

Figure 1: Hydraulic resistor. a) Symbolic representation b) Side-view of realized restrictions c) Cross section of realized restrictions d) Top view of a realized restriction.

For these triangular channels with a top width of $2w$ the resistance is given by:

$$R = \frac{17.4 \cdot L \cdot \mu}{w^4} \qquad (3)$$

The limits of the linear regime have been determined analytically and verified experimentally for liquids [7]. Entrance and exit effects result in a non-linear relation between p_{12} and ϕ_V . They can be neglected if the channel is long compared to the hydrodynamic entrance length. At low *Re* the entrance length L_{hy} increases linearly with *Re*. For circular channels with a diameter *d* this is expressed by [6]:

$$L_{hy} / d = 0.59 + 0.056 \cdot Re \qquad (4)$$

2.2 Hydraulic Capacitors

The hydraulic capacitor physically is an elastic membrane across which a pressure difference can be maintained. It is symbolically represented in fig. 2a. The capacitor establishes a relation between the pressure drop across the membrane and the displaced volume. For a linear capacitor the capacitance *C* is defined by:

$$C = \frac{V}{p_{12}} \qquad [N^{-1}m^5] \qquad (5)$$

Where *V* is the volume of the displaced liquid by bending of the membrane. Because the volume *V* is created by accumulation of the volume flow, (5) can be rewritten to find a relation between *effort* and *flow*:

$$\phi_V = C \cdot \frac{d}{dt} p_{12} \qquad (6)$$

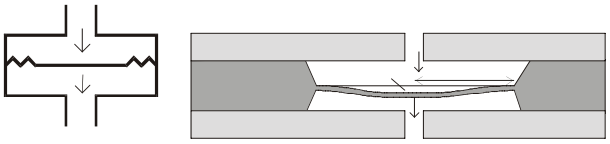

a) b)

Figure 2: Hydraulic capacitor a) Symbolic representation b) Cross section of a capacitor realized in glass-silicon-glass technology, showing the deflection of the membrane under influence of a pressure difference.

Fig. 2b shows a cross section of a capacitor realized in a glass-silicon-glass sandwich. For deflections smaller than the thickness of the membrane there is a linear relation between the applied pressure difference and the membrane deflection. In this case a simple expression for the capacitance can be derived:

$$C = \frac{\pi \cdot a^6}{192 \cdot D} \qquad [N^{-1}m^5] \qquad (7)$$

Where *a* is the radius of the membrane, and *D* is the flexural rigidity of the membrane, defined by $D = E \cdot h^3 / 12 \cdot (1-\nu^2)$, in which *E* [Pa] is the Young's modulus, ν [-] the Poission's ratio, and *h* [m] the thickness of the membrane.

2.3. Hydraulic Inertances

The hydraulic inertance is related to the mass-inertia of the liquid plug in a tube, symbolically represented in fig. 3. The accumulation of momentum in the tube under influence of a pressure difference is expressed by the balance equation:

$$\frac{d}{dt} \tilde{A} = p_{12} \qquad (8)$$

The stored momentum can be related to the volume flow by the buffer characteristic:

$$\tilde{A} = I \cdot \phi_V \qquad (9)$$

In which *I* is the inertance [Ns^2m^{-5}]. Combination of (8) and (9) gives the relation between *effort* and *flow*:

$$p_{12} = I \cdot \frac{d}{dt} \phi_V \qquad (10)$$

Figure 3: Symbolic representation of the hydraulic inertance.

For a liquid plug in a channel of lenght *L* and cross sectional area *A* the inertance equals:

$$I = \frac{\rho \cdot L}{A} \qquad (11)$$

Where ρ is the density of the liquid.

3 HYDRAULIC RELAXATION OSCILLATOR

Fig. 4 shows the schematic of a hydraulic astable multivibrator. It consists of a series connection of two inverting amplifiers and two relaxation coupling networks . The two inverting amplifiers are represented by PCV_1, R_5 and by PCV_2, R_6. The two RC relaxation networks are represented by R_1, R_2, C_1 and R_3, R_4, C_2. Hydraulic 'transistors' are implemented by means of a pressure controlled membrane valve (PCV). In the schematic shown in fig. 4 the transistors PCV_1 and PCV_2 should have a low resistance (open state) when the control pressure is low, in analogy with p-MOS (Metal-Oxide-Semiconductor) transistors.

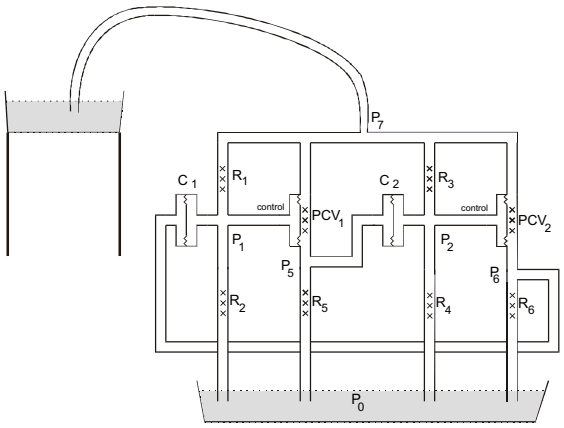

Figure 4: Schematic of a hydraulic astable multivibrator, composed of hydraulic resistors, capacitors and 'transitors'.

3.1 Hydraulic Inverting Amplifier

Fig. 5 shows a cross section of the pressure controlled valve. It is also realized in a glass-silicon-glass sandwich technology. The membrane deflects elastically under influence of the pressure differences p_{13} and p_{23}.

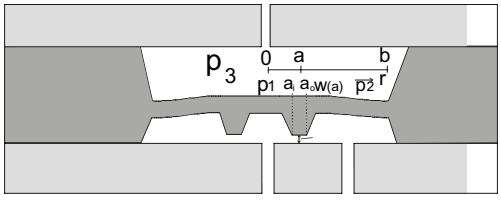

Figure 5: Cross section of the circular symmetrical membrane valve, realized in glass-silicon-glass technology. $w(a)$ is the membrane deflection at $r = a$, which gives the valve opening.

For small deflections the conductance G_{21} (= 1 / R_{21}) can be expressed as a function of the valve opening [8]:

$$G_{21}(p_{12}, p_{23}) = \frac{\pi \cdot w^3(a, p_{13}, p_{23})}{6 \cdot \mu \cdot \ln(\frac{a_o}{a_i})} \qquad [N^{-1}s^{-1}m^5] \qquad (12)$$

Where a_o is the outer and a_i is the inner radius of the valve seat. The valve opening ($w(a)$ in fig. 5) is a function of the applied pressure and the effective membrane stiffness k_1 and k_2:

$$w(a, p_{13}, p_{23}) = \frac{p_{13}}{k_1} + \frac{p_{23}}{k_2} \qquad (13)$$

A detailed valve model, including analytical expressions for k_1 and k_2 is given in [7]. For a silicon membrane with a radius b = 4 mm, a valve seat radius a = 0.96 mm and a thickness of 42 ± 1 µm, the measured values for the membrane stiffness are k_1 = 2.1 ± 0.2 x 10^9 Pa·m^{-1} and k_2 = 3.7 ± 0.2 x 10^8 Pa·m^{-1}. Using these values there is a good agreement between the measured G_{21} and eq. (12) [4, 7]. To improve the model for small valve openings, a parasitic leakage resistance R_{leak} = 1.4 ± 0.1 x 10^{12} N·s·m^{-5} was included.

The pressure controlled valves $PCV_{1,2}$ in combination with the resistors $R_{5,6}$ form two inverting amplifiers. The values $R_{5,6}$ (table 1) are chosen in between the closed and wide-open resistance of the PCV's. Fig. 6 shows the pressure transfer of a realized hydraulic invertor. There is a region (4 kPa< p_in < 7 kPa) where input variations are amplified (|slope| > 1). This is required to obtain oscillating behaviour of the astable multivibrator.

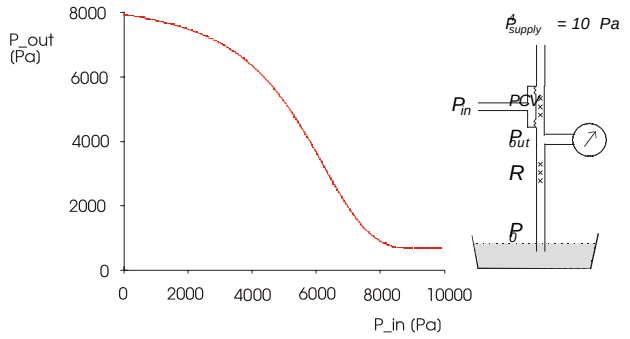

Figure 6: Measured pressure transfer of an inverting amplifier, consisting of a PCV and R = 2 x 10^{11} [N·s·m^{-5}].

3.2 Oscillator System Behaviour

All components from the schematic fig. 4 were realized in glass-silicon-glass technology on a single wafer, and connected by plastic tubes (fig. 7). The frequency of oscillation is determined by the relaxation time-constants R1//R2·C1 and R3//R4·C2. The values chosen for the resistors are listed in table 1, including the size of the triangular resistor channels. For the capacitors $C_{1,2}$ a value of 1 x 10^{-12} N^{-1}m^5 was chosen, which corresponds with a silicon membrane radius of 6.5 mm in combination with a 42 µm thickness. Together with the resistor values chosen a oscillation frequency of 0.16 Hz was predicted by network simulation [4]. The multivibrator was tested successfully, driven by a constant ethanol pressure of 0.1 bar (fig. 8). The measured free-running oscillation frequency was 0.18 Hz, in good agreement with the prediction.

Table 1: Resistor values and sizes

Resistor	Value [Nsm^{-5}]	Length [mm]	TopWidth 2w [µm]
$R_{1,2,3,4}$	1x10^{13}	6	118
$R_{5,6}$	2x10^{11}	6	316

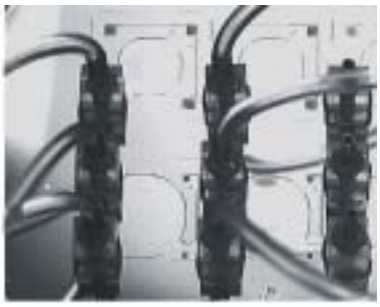

Figure 7: Photograph of the hydraulic relaxation oscillator realized.

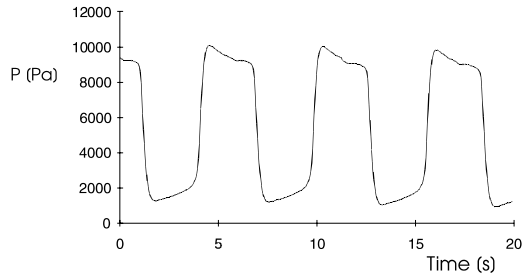

Figure 8: the measured output pressure (p_6 in fig. 4) of the free-running oscillator driven by a constant 0.1 bar pressure of ethanol.

4 SCALING

Based on the component descriptions, the scaling behaviour of hydraulic systems containing inertances, linear resistors and capacitors can be analysed. An important question is if these systems can be made faster by making them smaller. For this class of systems there are two types of characteristic time constants: For the filling of a hydraulic capacitance through a resistive channel the $R{\cdot}C$ time constants, and for the acceleration of the liquid in a resistive channel the I / R time constants. For a system S' that is λ times smaller than a system S in all three dimensions scaling laws have been derived for two cases.

4.1 Constant pressure with decreasing size

Down-scaling all dimensions λ times, including the capacitor membrane thickness corresponds with $\boldsymbol{p' = p}$. For the resistive filling it follows from eq. (2) and (7) that $R' = R{\cdot}\lambda^3$, $C' = C / \lambda^3$ therefore $(R{\cdot}C)' = R{\cdot}C$. For the acceleration of the liquid it follows from eq. (2) and (11) that $I' = \lambda I$, $R' = R{\cdot}\lambda^3$ therefore $(I/R)' = (I/R) / \lambda^2$. The liquid in the smaller channels tends to reach the stationary value quicker. However, the analysis of the $R{\cdot}C$-time constants shows that due to the increasing viscous resistance, smaller hydraulic systems containing capacitances will not be quicker. Therefore, to make smaller hydraulic systems quicker higher pressures are required to compensate for the viscous losses. This we have worked out in the next paragraph.

4.2 Down-Scaling with Increasing Pressure

Smaller $R{\cdot}C$ time-constants can be obtained by increasing the stiffness of capacitor membranes. We therefore propose to down-scale all dimensions λ times, except the membrane thickness. If the membrane thickness scales down with $\lambda^{2/3}$ we find $C' = C / \lambda^5$ and therefore $(R{\cdot}C)' = (R{\cdot}C) / \lambda^2$. Because $V' = V / \lambda^3$, it follows from eq. (5) that the pressure scales with $\boldsymbol{p' = p\lambda^2}$. Again for the inertance related relaxation we find $(I/R)'=(I/R)/\lambda^2$. Both time-constants scale down with λ^2, which implies that if pressures increase with decreasing size hydraulic systems indeed can be made quicker. For liquids there is the practical limit caused by the compressibility, giving a parasitic capacitance which inevitably scales with $C' = C/\lambda^3$. The related $R{\cdot}C$ time-constant does not scale-down with size.

5 CONCLUSIONS

The lumped network approach offers a powerful design and analysis tool for low Re hydraulic systems. We have illustrated this by rebuilding a common electronic relaxation oscillator in the hydraulic domain. The hydraulic astable multivibrator was successfully driven at a pressure of 10^4 Pa with ethanol as the medium. The analysis of the down-scaling of micro-hydraulic systems shows that to make smaller systems quicker, higher pressures are required to compensate for the viscous losses. However, a practical limit is caused by the compressibility of the liquid, which causes a $R{\cdot}C$ time-constant, which does not scale down with size.

REFERENCES

[1] H.M. Paynter, "Analysis and design of engineering systems", MIT Press, Cambridge (Mass.), 1961.

[2] P.C. Breedveld,"Physical Systems Theory in Terms of Bondgraphs", Ph.D. Thesis, University of Twente, 1984.

[3] F.C.M. van de Pol et al., Sensors and Actuators, A21-23, 1990, pp. 1052-1055.

[4] T.S.J. Lammerink et al., Proc. IEEE MEMS Conf., Amsterdam, The Netherlands, Jan. 29 – Febr. 2, 1995, pp. 13 – 18.

[5] R.E. Oosterbroek et al., Sensors and Actutors, 77, (1999), pp. 167 – 177.

[6] R.K. Shah, A.K. London, "Laminar flow forced convection in ducts", Ac. Press, New York, 1993.

[7] N.R.Tas,"Design and realization of a micromachined hydraulic astable multivibrator", M. Sc. Thesis University of Twente, 1994, ref. 070.6053.

[8] F.C.M van de Pol.,"A pump based on micro-engineering techniques", Ph.D. Thesis University of Twente, 1989.